

## First-principles study of magnetic properties in V-doped ZnO

Qian Wang<sup>a)</sup>

School of Physical Science and Technology, Southwest University, Chongqing 40071, China  
and Department of Physics, Virginia Commonwealth University, Richmond, Virginia 23284

Qiang Sun

Department of Advanced Materials and Nanotechnology, Peking University, Beijing 100871, China  
and Department of Physics, Virginia Commonwealth University, Richmond, Virginia 23284

Puru Jena

Department of Physics, Virginia Commonwealth University, Richmond, Virginia 23284

Zheng Hu

School of Chemistry and Chemical Engineering, Nanjing University, Nanjing 210093, China

R. Note and Y. Kawazoe

Institute for Materials Research, Tohoku University, Sendai 980-8577 Japan

(Received 3 February 2007; accepted 13 July 2007; published online 8 August 2007)

A comprehensive theoretical study of electronic and magnetic properties of V-doped ZnO in bulk as well as (11 $\bar{2}$ 0) thin films has been performed using density functional theory. Vanadium atoms substituted at Zn sites show very little selectivity of site occupancy. More importantly, different geometries with ferromagnetic, ferrimagnetic, and antiferromagnetic configurations are found to be energetically nearly degenerate both in Zn<sub>1-x</sub>V<sub>x</sub>O bulk and subsurface layers of the thin film. On the other hand, V atoms couple ferromagnetically when they occupy surface sites of the thin film. The diverse magnetic behaviors in V-doped ZnO account for the many reported conflicting experimental results. © 2007 American Institute of Physics. [DOI: 10.1063/1.2768628]

Transition metal-doped II–VI dilute magnetic semiconductor materials have been widely studied as these systems have many unique magneto-optical, magnetoelectrical, and magnetotransport properties. In addition, ferromagnetic (FM) coupling between the transition metal atoms may further enhance their applications in spintronic devices. Recently, several groups have experimentally studied the magnetic properties in (Zn, V)O systems.<sup>1–10</sup> However, the results are rather controversial. Saeki and co-workers<sup>1,2</sup> observed the FM behavior with a Curie temperature higher than 350 K while Hong *et al.*<sup>3,4</sup> found the room-temperature ferromagnetism along with a spin-glass-like behavior at low temperatures. Meanwhile, Venkatesan *et al.*<sup>5</sup> and Neal *et al.*<sup>6</sup> have, respectively, reported the observation of anisotropic ferromagnetism and room-temperature ferromagnetism in V-doped ZnO thin films. The latter authors<sup>6</sup> also reported paramagnetism at 10 K when the sample was subjected to rapid thermal annealing which agrees with the results of Saeki *et al.*<sup>7</sup> On the other hand, Ramachandran *et al.*<sup>8</sup> have reported that the Zn<sub>1-x</sub>V<sub>x</sub>O system does not exhibit any signature of ferromagnetism either at room temperature or at lower temperatures down to 10 K. Recent studies indicated the coexistence of Curie-Weiss paramagnetic (PM) and antiferromagnetic (AFM) V ions in ZnO thin films<sup>9</sup> and no pronounced ferromagnetism was observed down to 5 K in V-implanted ZnO single crystals.<sup>10</sup> These conflicting experimental results suggest that the magnetic coupling may be sensitive to sample preparation conditions and defects.

The theoretical results have been equally conflicting. For example, Sato and Katayama-Yoshida<sup>11</sup> found the ferromagnetism in V-doped ZnO using Korringa-Kohn-Rostoker co-

herent potential approximation with local density approximations, while Kang *et al.*<sup>12</sup> reported the antiferromagnetism in this system using the full-potential linear muffin-tin orbital method with generalized gradient approximation (GGA) for exchange-correlation energy. No theoretical study is available for Zn<sub>1-x</sub>V<sub>x</sub>O thin films or surfaces. In this letter, we present a systematic theoretical study of the electronic and magnetic properties of V-doped ZnO system in both bulk and thin films.

The total energy calculations and the geometry optimizations have been carried out using spin polarized density functional theory (DFT) and the PW91 form<sup>13</sup> for the GGA functional for exchange and correlation. A plane-wave basis set and the projector augmented wave potentials<sup>14</sup> were employed as implemented in the Vienna *ab initio* simulation package (VASP).<sup>15</sup> Calculations were performed by setting the convergence in energy and force at 10<sup>-4</sup> eV and 10<sup>-3</sup> eV/Å, respectively, and the cutoff energy at 320 eV for the plane-wave basis. The accuracy of our calculations has been well established for ZnO from our previous work.<sup>16–18</sup>

We begin our calculations with V-doped ZnO bulk for which a (3 × 3 × 2) supercell consisting of Zn<sub>36</sub>O<sub>36</sub> was used. We replaced two of the Zn atoms in the supercell with V atoms. This corresponds to a doping concentration of 5.6% and is consistent with the concentration studied in most experiments, namely, ~3%–15%. Since it is *a priori* not clear which Zn sites will be preferred by V in the supercell, we have considered six different configurations (see Fig. 1 and Table I). For each of these configurations, the geometry of the supercell (ionic coordinates and *c/a* ratio) was fully optimized without any symmetry constraint. The total energies, electronic structure, and magnetic moments on each V atom were calculated self-consistently for different spin align-

<sup>a)</sup>Electronic mail: qwang@vcu.edu

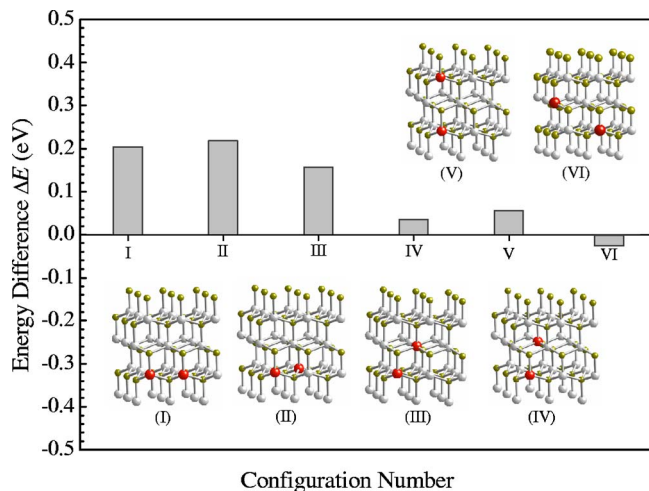


FIG. 1. (Color online) Energy differences,  $\Delta E = E_{\text{AFM}} - E_{\text{FM}}$ , for the six configurations of ZnO ( $3 \times 3 \times 2$ ) supercell with V doping. The lighter spheres are Zn, the darker spheres are O, and the bigger and red spheres are V.

ments (FM and AFM). The  $k$ -point convergence was achieved with a  $(5 \times 5 \times 5)$  Monkhorst-Pack grid.<sup>19</sup> The magnetic coupling for the pair of V atoms is determined from the total energy difference  $\Delta E$  between the FM and AFM states ( $\Delta E = E_{\text{AFM}} - E_{\text{FM}}$ ). The negative  $\Delta E$  means that the AFM state is lower in energy than the FM state.

Six configurations studied in this work can be classified into two subgroups: group 1 includes configurations I, II, and III (Fig. 1) where the two V atoms cluster around a bridging O atom in different directions, while the other three configurations belonging to group 2 have a larger V–V distance. From total energy calculations, we find that all three configurations in group 2 are nearly degenerate in energy, and they are slightly (30–80 meV) lower than those of the configurations in group 1. This clearly suggests that there is no clear site preference for the two V atoms in bulk ZnO. This is in agreement with experimental findings that V doping in ZnO is almost homogeneous.<sup>1–8</sup> The FM state in configurations

TABLE I.  $\Delta \varepsilon$  (in eV) is the relative energy with respect to the ground state configurations of IV and I for  $\text{Zn}_{34}\text{V}_2\text{O}_{36}$  (crystal) and  $\text{Zn}_{52}\text{V}_4\text{O}_{56}$  (thin film) supercells, respectively.  $\Delta E$  is the total energy difference between the AFM and FM states (in eV) for each configuration. The optimized V–V distance  $d_{\text{V-V}}$  (in Å) and magnetic moments (in  $\mu_B$ ) at V atom for all the configurations for  $\text{Zn}_{34}\text{V}_2\text{O}_{36}$  bulk supercell and  $\text{Zn}_{52}\text{V}_4\text{O}_{56}$  slab supercell are also given.

Configurations	$\Delta \varepsilon$	$\Delta E$	$d_{\text{V-V}}$	$\mu_{\text{V}}$
$\text{Zn}_{34}\text{V}_2\text{O}_{36}$				
I	0.051	0.204	3.299	1.905
II	0.065	0.218	3.249	1.900
III	0.078	0.157	3.282	1.876
IV	0.000	0.035	4.652	1.871
V	0.021	0.056	5.332	1.864
VI	0.020	-0.022	5.718	1.864
$\text{Zn}_{52}\text{V}_4\text{O}_{56}$				
I (2, 3/51, 50)	0.000	0.380	3.092	2.184
II (2, 7/51, 54)	0.162	-0.019	4.831	2.097
III (3, 7/50, 54)	0.119	-0.015	5.628	2.046
IV (2, 12/51, 44)	0.405	0.089	3.120	2.277
V (12, 13/44, 45)	0.552	0.021	3.205	1.850
VI (12, 16/44, 47)	0.538	-0.026	5.628	1.833

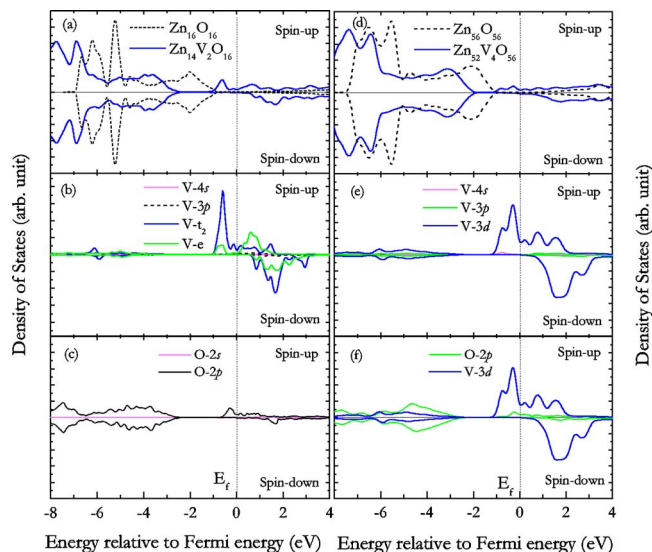


FIG. 2. (Color online) Calculated total and partial DOS for the ZnO ( $2 \times 2 \times 2$ ) bulk and the ( $2 \times 2$ ) thin film supercell with and without V doping.

I, II, and III in group 1 lies 0.204, 0.218, and 0.157 eV lower in energy than the AFM state, respectively. Note that in experiments, if the dopant configurations are similar to those of group 1, ferromagnetism would be observed.<sup>1–6</sup> In group 2, two of the FM states lie only 56 and 35 meV lower in energy than the corresponding AFM states, while in configuration VI the AFM state is lower in energy than the FM state by 22 meV. Since these energy differences are rather small, depending on experimental condition, one can expect that FM, PM, and AFM states are all possible in V-doped ZnO. This will account for the diverse magnetic behavior found in experiments.<sup>1–10</sup>

To study the effect of doping concentration, we generated a smaller ZnO ( $2 \times 2 \times 2$ ) supercell ( $\text{Zn}_{16}\text{O}_{16}$ ) and replaced two Zn atoms with V, corresponding to a 12.5% V doping concentration. We performed the calculations in the same way as described above for the ( $3 \times 3 \times 2$ ) supercell using the  $(6 \times 6 \times 6)$   $k$ -point mesh. Our conclusions regarding the site preference and magnetic coupling remain unchanged. It was found that the lowest energy configuration with two V atoms occupying the nearest-neighbor Zn sites in the (0001) plane is FM and lies 0.255 eV lower in energy than the AFM state. The other configurations are found to be 0.080–0.142 eV higher in energy than the FM ground state.

The electronic densities of states (DOS) of V-doped ZnO are plotted in Figs. 2(a)–2(c). The total DOS for the ground state configuration of the  $\text{Zn}_{0.875}\text{V}_{0.125}\text{O}$  supercell exhibits half-metallic character with an energy gap of 2.68 eV in the minority spin DOS. The DOS figures clearly show that when V atoms are incorporated into ZnO, they introduce new states either inside the valence band or above the valence band maximum (VBM). The V 3d orbitals split into  $t_2$  and  $e$  orbitals in a tetrahedral field of ZnO crystal structure and the O  $p$  orbitals have  $t_2$  symmetry. Therefore, the induced V  $t_2$  states above the VBM interact with the O  $p$  states, forming hybrid  $pd$  states. Figures 2(b) and 2(c) show that the metallic majority spin DOS at the  $E_F$  is mainly composed of V  $t_2$  and O  $2p$  states. This suggests that the hybridization between V  $t_2$  and O  $2p$  is responsible for the half-metallic behavior.

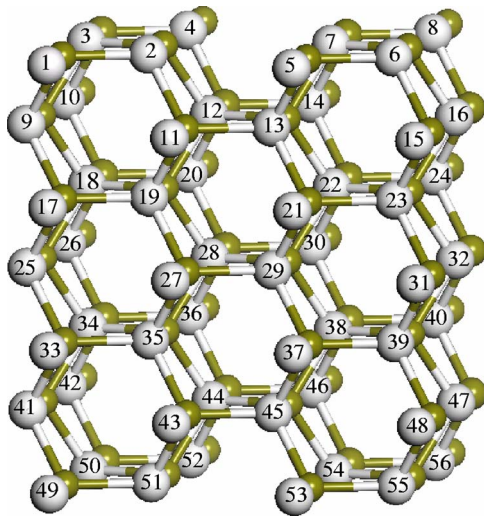


FIG. 3. (Color online) Supercell of the ZnO ( $11\bar{2}0$ ) slab consisting of 56 Zn and 56 O atoms. The numbered spheres represent Zn.

We now analyze V-doped ZnO thin films. The ZnO thin film was modeled by a  $(2 \times 2)$  seven-layer slab having a  $[11\bar{2}0]$  surface orientation and 56 f.u. of ZnO (see Fig. 3). Each slab was separated from another by a vacuum region of  $10 \text{ \AA}$  along the  $[11\bar{2}0]$  direction. The central three layers of the slab were held at their bulk position. Two layers on either side of the slab were taken to be identical to preserve symmetry and allowed to relax without any symmetry constraint. The surface reconstruction was carried out by using a  $5 \times 5 \times 1$   $k$ -point mesh. The calculated geometrical parameters and cohesive energies are in good agreement with our previous work on a smaller slab supercell.<sup>16</sup> To determine the preferred site of a V atom in the thin film, total energy calculations of supercells with a V atom residing on the surface and subsurface were carried out. The surface site is found to be  $0.02 \text{ eV}$  lower than that of the subsurface site. This energy difference is indeed very small, as compared to that in the (Ga, Mn)N thin films, where the Mn atom occupying the surface sites was found to lie  $1.37 \text{ eV}$  lower in energy than the subsurface sites.<sup>20</sup> Thus, one can conclude that V does not exhibit any site preference in ZnO thin films in the dilute limit. This is consistent with the experimental finding.<sup>1-8</sup>

The magnetic coupling between V atoms was studied by replacing two Zn atoms with V on either side of the slab. Hence, a total replacement of four Zn atoms with four V atoms resulted in  $7.14\%$  doping concentration and a  $\text{Zn}_{52}\text{V}_4\text{O}_{56}$  supercell. We have considered six configurations to simulate this replacement, which are specified in Table I by indicating the sites where the Zn atoms are substituted by V. Geometry optimization and total energy calculations corresponding to both FM and AFM states for all these six configurations were carried out to determine the most preferred geometrical and magnetic states. The results are again summarized in Table I.

Configuration I has the lowest energy configuration with FM state being  $0.38 \text{ eV}$  lower in energy than the AFM state. This is consistent with the known experiments.<sup>1-6</sup> However, when one V atom is in the surface layer and the other one is in subsurface layer (configuration IV), the energy difference between FM and AFM is reduced to  $0.089 \text{ eV}$ . When both of

the two V atoms are in the subsurface layer (configurations V and VI), this energy difference becomes even smaller, namely,  $0.021$  and  $-0.026 \text{ eV}$ , respectively. In these cases, FM and AFM states are almost degenerate, displaying a weak magnetism.

Figures 2(d)–2(f) show the total and partial spin DOS for the majority and minority electrons in the ground state configuration of the  $\text{Zn}_{56}\text{O}_{56}$  supercell with and without V doping. For the undoped case, the DOS curves for the majority or minority states are completely symmetric with a large energy gap, and  $E_f$  lies in the gap region. For the V-doped ZnO thin film, the total DOS shows half-metallic behavior with nearly  $100\%$  spin polarization, which is ideal for injection of spin polarized charge carriers into the nonmagnetic ZnO. We note that the induced new states appearing in the gap originate from the majority states of the V  $3d$  and O  $2p$  orbitals. There is a clear overlap between V  $3d$  and O  $2p$  orbitals near  $E_f$  which passes right through the gap in the spin-down DOS. This suggests that the double exchange mechanism is most likely responsible for the FM coupling in this system.<sup>21</sup>

In summary, we present extensive theoretical calculations of the magnetic properties of V-doped ZnO crystal and thin films using spin polarized DFT and the supercell method. We show that different magnetic configurations are nearly degenerate in energy in bulk  $\text{Zn}_{1-x}\text{V}_x\text{O}$ . However, the FM phase of the  $\text{Zn}_{0.93}\text{V}_{0.07}\text{O}$  thin film is energetically the most preferred state. The strong hybridization between V  $3d$  and O  $2p$  is found to be responsible for the FM coupling. Our theoretical results indicate that depending on experimental methods and doping concentration, intrinsically diverse magnetic coupling can exist in (Zn, V)O systems.

<sup>1</sup>H. Saeki, H. Tabata, and T. Kawai, Solid State Commun. **120**, 439 (2001).

<sup>2</sup>Y. Ishida, J. I. Hwang, M. Kobayashi, A. Fujimori, H. Saeki, H. Tabata, and T. Kawai, Physica B **351**, 304 (2004).

<sup>3</sup>N. Hong, J. Sakai, and A. Hassini, J. Appl. Phys. **97**, 10D312 (2005).

<sup>4</sup>N. Hong, J. Sakai, and A. Hassini, J. Phys.: Condens. Matter **17**, 199 (2005).

<sup>5</sup>M. Venkatesan, C. B. Fitzgerald, J. G. Lunney, and J. M. D. Coey, Phys. Rev. Lett. **93**, 177206 (2004).

<sup>6</sup>J. R. Neal, A. J. Behan, R. M. Ibrahim, H. J. Blythe, M. Ziese, A. M. Fox, and G. A. Gehring, Phys. Rev. Lett. **96**, 197208 (2006).

<sup>7</sup>H. Saeki, H. Matsui, T. Kawai, and H. Tabata, J. Phys.: Condens. Matter **16**, S5533 (2004).

<sup>8</sup>S. Ramachandran, A. Tiwari, J. Narayan, and J. T. Prater, Appl. Phys. Lett. **87**, 172502 (2005).

<sup>9</sup>Y. Ishida, J. I. Hwang, M. Kobayashi, Y. Takeda, K. Mamiya, J. Okamoto, S. I. Fujimori, T. Okane, T. K. Terai, Y. Saitoh, Y. Muramatsu, A. Fujimori, A. Tanaka, H. Saeki, T. Kawai, and H. Tabata, Appl. Phys. Lett. **90**, 022510 (2007).

<sup>10</sup>S. Zhou, K. Potzger, H. Reuther, K. Kuepper, W. Skorupa, M. Helm, and J. Fassbender, J. Appl. Phys. **101**, 09H109 (2007).

<sup>11</sup>K. Sato and H. Katayama-Yoshida, Semicond. Sci. Technol. **17**, 367 (2002).

<sup>12</sup>B. S. Kang, W. C. Kim, Y. Y. Shong, and H. J. Kang, J. Cryst. Growth **287**, 74 (2006).

<sup>13</sup>Y. Wang and J. P. Perdew, Phys. Rev. B **44**, 13298 (1991).

<sup>14</sup>G. Kresse and J. Joubert, Phys. Rev. B **59**, 1758 (1999).

<sup>15</sup>G. Kresse and J. Furthmüller, Phys. Rev. B **54**, 11169 (1996).

<sup>16</sup>Q. Wang and P. Jena, Appl. Phys. Lett. **84**, 4170 (2004).

<sup>17</sup>Q. Wang, Q. Sun, B. K. Rao, and P. Jena, Phys. Rev. B **69**, 233310 (2004).

<sup>18</sup>Q. Wang, Q. Sun, P. Jena, and Y. Kawazoe, Phys. Rev. B **70**, 052408 (2004).

<sup>19</sup>H. J. Monkhorst and J. D. Pack, Phys. Rev. B **13**, 5188 (1976).

<sup>20</sup>Q. Wang, Q. Sun, P. Jena, and Y. Kawazoe, Phys. Rev. Lett. **93**, 155501 (2004).

<sup>21</sup>H. Akai, Phys. Rev. Lett. **81**, 3002 (1998).